INTERNATIONAL JOURNAL FOR NUMERICAL METHODS IN FLUIDS, VOL. 27, 229–239 (1998)

NEW FINITE-ELEMENT-BASED FLUCTUATION-SPLITTING KINETIC SCHEMES

BRAHIM KHOBALATTE[1,2] AND PÉNÉLOPE LEYLAND[2]*

[1]Von Karman Institute for Fluid Dynamics, Chaussée de Waterloo 72, B-1640 Rhode Saint-Genèse, Belgium.
[2]Institute de Machines Hydraliques et Mécanique des Fluids, Ecole Polytechnique Fédérale de Lausanne, CH-1015 Lausanne, Switzerland

SUMMARY

Starting from the gas kinetic model, a new class of schemes for hyperbolic systems of conservation laws is presented. The flow solvers are based on the Boltzmann equations. The numerical discretization is based on the upwind cell vertex fluctuation-splitting model. The method is truly multidimensional in the sense that the splitting is independent of a particular normal direction; the geometry of the mesh does not influence the upwinding. Numerical results for inviscid flow test cases are presented to indicate the robustness and accuracy of the schemes. © 1998 John Wiley & Sons, Ltd.

Int. J. Numer. Meth. Fluids, **27**, 229–239 (1998)

KEY WORDS: kinetic approach; finite element schemes; Euler equations; hyperbolic systems

1. INTRODUCTION

Fluctuation-splitting space discretization schemes have been introduced and developed for the last few years for scalar advection equations. Their extension to multidimensional non-linear transport equations is non-trivial owing to the complex wave decompositions involved.[1] Since the Euler equations can be derived directly from the zeroth-order moments of the Boltzmann equations written as free transport equations, one way to use these schemes for such non-linear conservation laws is the kinetic approach. In this paper the kinetic approach is used to solve the compressible Euler equations using the above-mentioned new schemes for unstructured triangular meshes. This allows us to extend these schemes to the multidimensional case and gives conservative, stable, positive and entropy-satisfying finite element schemes. This approach has been investigated by a number of authors for finite-volume-type schemes.[2–6] However, for the case of 'fluctuation-splitting' schemes the equilibrium state is considered to be a Maxwellian one and the triangulations must be deduced from quadrilaterals.[7] By simplifying this function, this can be extended to any kind of triangulation.[8,9] However, the integrals involved limit the practical feasibility to equivalent first-order schemes, which nevertheless give remarkably good results. The development of these schemes in a truly compact finite element approach, maintaining the properties of positivity, stability and entropy preservation, is presented here and extensions to second order are possible by simplifying the Maxwellian-type distribution by Dirac ones. The tedious integrals that were necessary before become redundant and

*Correspondence to: P. Leyland, IMHEF, EPFL, CH-1015 Lausanne, Switzerland.

CCC 0271–2091/98/010229–11 $17.50 *Received May 1996*

the resulting schemes maintain at least precision, entropy and stability. Three classes of fluctuation-splitting schemes are considered, the so-called N-scheme, which in spite of its low spatial order (0·8) is always positive and gives comparable results to the higher-order (1·6) so-called PSI scheme, and another linear decomposition scheme which is non-positive, LDA. For PSI and LDA, only Dirac distributions are used; for the N-scheme, comparisons of different approximate equilibrium distributions are made.

For transonic and supersonic compressible flows all the above schemes proved to give accurate representations of several difficult flow situations. The numerical results presented here consist of a number of steady and unsteady shock–shock interaction and shock reflection test cases, such as the supersonic scramjet inlet presented below, where the multiple shock reflections and geometry-induced expansion fans are captured with high accuracy on a relatively coarse finite element triangular unstructured mesh.

2. KINETIC APPROACH

The approach presented here is based on the dynamical theory of gases rather than the conservative formulation of the Euler or Navier–Stokes equations. As is well known, these equations can be derived from the Boltzmann equations, which can be written as conservation transport equations for the molecular distribution function $f(\bar{x}, t, \bar{v}, I)$, where $\bar{x}$ denotes the relative position, $\vec{v}$ the microscopic velocity and I the internal energy:

$$\partial_t f + \vec{v} \cdot \nabla f = \frac{1}{\epsilon} \mathcal{Q}_s(f). \tag{1}$$

The right-hand side represents the intermolecular collision operator and ϵ is the Knudsen number.

The local translational equilibrium state is described by a scalar advection equation with an identically zero collision integral for f given by a generalized Maxwellian distribution function f_0:

$$\partial_t f_0 + \vec{v} \cdot \nabla f_0 = 0. \tag{2}$$

For totally elastic collisions we have conservation of density, momentum and total energy. The conservation equations are thus the approximations obtained by taking the moments of the Boltzmann equations with respect to the collision vector $(1, \vec{v}, \|\vec{v}\|^2/2 + I^\delta)^{\mathrm{T}}$, where δ is a parameter related to the thermodynamic state equation of the system.

Multiplying (1) by the collision vector $(1, \vec{v}, \|\vec{v}\|^2/2 + I^\delta)^{\mathrm{T}}$ and integrating in the space spanned by $\mathrm{d}\vec{v}$ and $\mathrm{d}I$, we obtain the system of conservation laws:

$$\partial_t W + \operatorname{div} F(W) = 0 \quad \text{in } \Omega \times \mathbb{R}^+, \tag{3}$$

where W is the vector of conserved variables and F is the flux, given by

$$W = \begin{bmatrix} \rho \\ \rho\vec{u} \\ E \end{bmatrix}, \qquad F(W) = \begin{bmatrix} \rho\vec{u} \\ \rho\vec{u} \otimes \vec{u} + \tau \\ (E + \tau)\vec{u} + q \end{bmatrix}. \tag{4}$$

By taking f to be the locally Maxwellian equilibrium distribution and by taking first-order moments of (1) with respect to the collision vector, the system (3) is reduced to the compressible Euler equations with

$$\tau = \rho T \mathbb{I}_N \equiv p \mathbb{I}_n, \qquad q = 0, \qquad E = \frac{\rho}{2}|\vec{u}|^2 + \frac{\rho T}{\gamma - 1}, \quad 1 \le \gamma \le 2.$$

Kinetic schemes for the Euler equations are thus based upon moments of the discretised Boltzmann equations by approaching (3) by a fractional step method. Several authors have employed this approach with considerable success using finite volume schemes and a Maxwellian distribution function (see e.g. References 2–6). For finite-element-type schemes this analysis has been restricted to rectangular grids or triangular ones derived from quadrilaterals.[7] By introducing velocity distributions with compact support, this stage was advanced in References 3 and 4 by allowing the same analysis on arbitrary grids.

This kinetic approach, written here in two dimensions, considers the free transport equation:

$$\partial_t F + \vec{v}\nabla_{\vec{x}} F = 0, \quad t \in [t^n, t^{n+1}], \quad (\vec{x}, \vec{v}) \in \Omega \times \mathbb{R}^2, \tag{5}$$

with initial condition

$$F(x, \vec{x}, t)|_{t=t^n} = F^n(x, \vec{v}) \quad \text{for all } (x, \vec{v}) \in \Omega \times \mathbb{R}^2.$$

For the initial condition of (3), $(\rho^n, \vec{u}^n, T^n)$, the function F^n is given by

$$F^n(x, \vec{v}) = (f^n(x, \vec{v}), g^n(x, \vec{v})),$$

where the data f and g are of the form

$$f^n(x, \vec{v}) = \frac{\rho^n(x)}{T^n}\chi\left(\frac{\vec{v} - \vec{u}^n(x)}{\sqrt{T^n(x)}}\right), \qquad g^n(x, \vec{v}) = \rho^n(x)\psi\left(\frac{\vec{v} - \vec{u}^n(x)}{\sqrt{T^n(x)}}\right),$$

with a particular choice for χ and ψ such that the free transport equations in f and g are related to (3) via

$$W^n \equiv \begin{pmatrix} \rho^n \\ \rho^n \vec{u}^n \\ E^n \end{pmatrix} = \int_{\vec{v}\in\mathbb{R}^2} [V_1(\vec{v}) f(\vec{v}) + V_2 g(\vec{v})] \, \mathrm{d}\vec{v},$$

$$\mathscr{F}(W^n) \equiv \begin{pmatrix} \rho^n \vec{u}^n \\ \rho^n \vec{u}^n \otimes \vec{u}^n + p^n \mathbb{I}_N \\ (E^n + p^n)\vec{u}^n \end{pmatrix} = \int_{\vec{v}\in\mathbb{R}^2} \vec{v}[V_1(\vec{v}) f(\vec{v}) + V_2 g(\vec{v})] \, \mathrm{d}\vec{v},$$

where the collision vectors $V_1(\vec{v})$ and V_2 are defined as

$$V_1(\vec{v}) = \begin{pmatrix} 1 \\ \vec{v} \\ |\vec{v}|^2/2 \end{pmatrix}, \qquad V_2 = \begin{pmatrix} 0 \\ \vec{0} \\ 1 \end{pmatrix}.$$

This is the key point: use recent advances in new multidimensional schemes[1] for scalar advection equations to solve the transport equation for F, (5), and in this way these schemes can be used to solve the system of conservation laws, (3), via the kinetic approach.

Several choices of χ and ψ are possible. In particular, the following have been studied in References 2, 3 and 5–7:

$$\chi(\vec{\omega}) = \frac{1}{2\pi}\exp\left(-\frac{|\vec{\omega}|^2}{2}\right), \qquad \psi(\vec{\omega}) = \lambda\chi(\vec{\omega}),$$

where λ is related to the ratio of specific heats γ in the state equation via

$$\lambda = \frac{2 - \gamma}{\gamma - 1}.$$

These functions can be further approximated by replacing them by simpler compact support distributions[3,4,9] such as a circular (2D)/spherical (3D) one, i.e.

$$\chi(\vec{\omega}) = \frac{1}{4\pi} 1_{|\vec{\omega}|\sqrt{2}}, \qquad \psi(\vec{\omega}) = \lambda\chi(\vec{\omega}), \tag{6}$$

or a rectangular/Heaviside shape, i.e.

$$\chi(\vec{\omega}) = \tfrac{1}{12} 1_{\{|\omega_1|\leq\sqrt{3}\}} 1_{\{|\omega_2|\leq\sqrt{3}\}}, \qquad \psi(\vec{\omega}) = \lambda\chi(\vec{\omega}). \tag{7}$$

Finally, the Dirac distribution, often used in probabilistic resolutions of the Boltzmann equations, can also be employed:

$$\chi(\vec{\omega}) = \tfrac{1}{4} \sum_{(i,j)\in\mathscr{E}} \delta_{\vec{\omega}=(i,j)}, \qquad \psi(\vec{\omega}) = \lambda\chi(\vec{\omega}), \tag{8}$$

where

$$\mathscr{E} = \{(1, 1), (-1, 1), (1, -1), (-1, -1)\}$$

and $\delta_{\vec{\omega}=\vec{e}}$ denotes the Dirac distribution at $\vec{e}$.

All the above functions χ and ψ are non-negative functions satisfying

$$\int_{\vec{\omega}\in\mathbb{R}^2} \begin{pmatrix} 1 \\ \omega_i\omega_j \end{pmatrix} \chi(\vec{\omega}) \mathrm{d}\vec{\omega} = \begin{pmatrix} 1 \\ \delta_{i,j} \end{pmatrix}, \qquad \int_{\vec{\omega}\in\mathbb{R}^2} \psi(\vec{\omega})\ \mathrm{d}\vec{\omega} = \lambda, \tag{9}$$

where $\delta_{i,j}$ denotes the Kronecker symbol.

3. MULTIDIMENSIONAL WEIGHTED RESIDUAL SCHEMES

Upwind Riemann solvers with finite volume schemes for compressible flows have been developed and applied for the last 15 years on structured and unstructured meshes. However, they are often based upon a monodimensional approach along the normal direction out of the computational cell. This direction is explicitly part of the numerical flux function, thus leading to grid dependence. Multidimensional upwind schemes have also been developed during the last 5 years, but they often involve highly complex wave decompositions. Since Boris and Book many years ago,[10] who used weighted residual schemes[11] for compressible flow solvers with finite elements, considerable progress is now being made in this alternative multidimensional approach. The numerical residuals per cell (element) are distributed by some scheme within the cell to the nodes, this distribution defining the numerical flux.

We assume that the computational domain Ω is a polygonal bounded domain in $\mathbb{R}^d$, $d=2,3$. Let $\mathscr{T}_h$ be a triangulation of Ω. For the schemes studied here, the following notation is introduced.

The nodes of $\mathscr{T}_h$ are ($i=1,\ldots,ns$) and for each triangle T of $\mathscr{T}_h$ we will generically call (i, j, k) its vertices. $\vec{n}_i \equiv \vec{n}(i, T)$ is the inward normal of T opposite to the summit $\vec{x}_i$, with length $|\vec{x}_j - \vec{x}_k|$.

Then, considering the discretization of equations (3) on Ω, nodal values are updated as

$$W_i^{n+1} = W_i^n + \frac{\Delta t_i^n}{|C_i|} \sum_{\{T/i\in T\}} \Phi_T^i, \tag{10}$$

where Φ_T^i is the contribution of the numerical flux function (fluctuation splitting) per element T to node i. $|C_i|$ denotes the volume of the topological dual cell around node i. W_i^n represents the average of W at time $t^n = n\Delta t_i^n$ within the cell. The exact flux Φ_t in every triangle T, i.e.

$$\Phi_T = \int_{\partial T} \mathscr{F}(W(t^n, x))\vec{n}\, \mathrm{d}x, \tag{11}$$

where ∂T defines the surface of cell T with inward normal $\vec{n}$, is replaced by a simple function

$$\Phi_T^i = -\tfrac{1}{2}[\mathscr{F}_T^i(w_i^n)\vec{n}_i + \mathscr{F}_T^i(w_j^n)\vec{n}_j + \mathscr{F}_T^i(w_k^n)\vec{n}_k] \tag{12}$$

called the residual distribution, where the functions $\mathscr{F}_T^i$ are calculated such that Φ_T^i gives a conservative scheme (10); that is, for every triangle $T \in \mathscr{T}_h$,

$$\Phi_T^i + \Phi_T^j + \Phi_T^k = \Phi_T \tag{13}$$

for (i, j, k)—the three nodes of triangle T.

We have used in this study a Boltzmann solver. The functions $\mathscr{F}_T^i$ are given by

$$\mathscr{F}_T^i(W) = \frac{\rho}{T}\int_{\vec{v}\in\mathbb{R}^2} \vec{v}\left[V_1(\vec{v})\beta_T^i\chi\left(\frac{\vec{v}-\vec{u}}{\sqrt{T}}\right) + V_2\tilde{\beta}_T^i T\psi\left(\frac{\vec{v}-\vec{u}}{\sqrt{T}}\right)\right] \mathrm{d}\vec{v}, \tag{14}$$

where β_T^i and $\tilde{\beta}_T^i$ are the coefficient distributions associated with the transport equations for f and g respectively and which, by conservativity, satisfy, for all $T \in \mathscr{T}_h$,

$$\beta_T^i + \beta_T^j + \beta_T^k \equiv \tilde{\beta}_T^j + \tilde{\beta}_T^k = 1. \tag{15}$$

4. FLUCTUATION-SPLITTING SCHEMES FOR FINITE ELEMENTS WITH KINETIC APPROACH

Following References 1, 12 and 13, the fluctuation-splitting schemes on triangular finite element meshes for the advection equations (5) are given by

$$F_i^{n+1} = F_i^n + \frac{\Delta t^n}{|C_i|}\sum_{\{T/i\in T\}} \vec{\phi}_T^i, \tag{16}$$

with $\vec{\phi}_T^i = [\phi_T^i, \tilde{\phi}_T^i]$, where

$$\phi_T^i = -\tfrac{1}{2}\beta_T^i\vec{v}\cdot(\vec{n}_i f_i^n + \vec{n}_j f_j^n + \vec{n}_k f_k^n) \equiv \beta_T^i\phi_T,$$

$$\tilde{\phi}_T^i = -\tfrac{1}{2}\tilde{\beta}_T^i\vec{v}\cdot(\vec{n}_i g_i^n + \vec{n}_j g_j^n + \vec{n}_k g_k^n) \equiv \tilde{\beta}_T^i\tilde{\phi}_T$$

and β_T^i and $\tilde{\beta}_T^i$ are the coefficient distributions satisfying (15).

The scheme (16) is upwind in the sense that no flux contribution is sent to upstream nodes, i.e.

$$\beta_T^i \equiv \tilde{\beta}_T^i = 0 \quad \text{if } \vec{v}\cdot\vec{n}_i < 0. \tag{17}$$

Figure 1 shows the two possible situations that can occur. In case (a) there is only one inflow side and the entire fluctuation flux is sent to the unique downstream node i, (one-inflow case: $\vec{v}\cdot\vec{n}_i > 0,\ \vec{v}\cdot\vec{n}_j < 0\ \vec{v}\cdot\vec{n}_k < 0$), i.e.

$$\beta_T^i \equiv \tilde{\beta}_T^i = 1, \qquad \beta_T^j \equiv \tilde{\beta}_T^j = 0, \qquad \beta_T^k \equiv \tilde{\beta}_T^k = 0. \tag{18}$$

In case (b) the fluctuation flux is split between the two nodes i and j, (two-inflow case:$\vec{v}\cdot\vec{n}_i > 0,\ \vec{v}\cdot\vec{n}_j > 0, \vec{v}\cdot\vec{n}_k < 0$). The way in which these coefficients are evaluated determines the properties of the scheme, the most important of these being the positivity and linearity preservation.

A linearity-preserving scheme is such that the distribution coefficients β_T^i are bounded. In this case, when the cell residual Φ_T tends to zero, the contributions $(\phi_T^\alpha,\ \alpha = i, j, k)$ also tend to zero. This property yields a second-order-accurate solution at steady state.

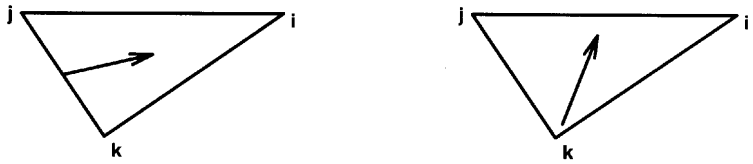

Figure 1. Two different kinds of upwinded triangles

4.1. N-scheme

This first class of schemes was introduced in References 13 and 14. They are linear, positive and entropy-preserving. For finite-difference-type structured grids they produce the narrowest stencil. The scheme only sends a flux contribution to downstream vertices. Thus the distribution coefficients for the two-inflow case (i, j) are given by

$$\beta_T^i \equiv \beta_T^{\mathrm{N},i} = \frac{\phi_T^i}{\phi_T}, \qquad \beta_T^j \equiv \beta_T^{\mathrm{N},j} = \frac{\phi_T^j}{\phi_T},$$

where

$$\phi_T^i = -\tfrac{1}{2}\vec{v}\cdot\vec{n}_i(f_i^n - f_k^n), \qquad \phi_T^j = -\tfrac{1}{2}\vec{v}\cdot\vec{n}_j(f_j^n - f_k^n),$$

and for the one-inflow case we have the relation (18).

4.2. LDA-scheme

The LDA (low-diffusion A) scheme is a linearity-preserving second-order scheme which is not positive. The distribution coefficients are given by

$$\beta_T^i \equiv \beta_T^{\mathrm{LDA},i} = \frac{\max(0, \vec{v}\cdot\vec{n}_i)}{\sum_{\alpha=i,j,k}\max(0, \vec{v}\cdot\vec{n}_\alpha)}. \tag{19}$$

As this scheme is not positive, it can produce oscillations in high-gradient regions of the flow.

4.3. PSI scheme

In order to combine both positivity and linearity preservation, one has to look for non-linear schemes such as the PSI scheme, which is considered in Reference 13 to be the best-performing non-linear fluctuation-splitting scheme and whose compact formula reads[1,13]

$$\beta_T^i \equiv \beta_T^{\mathrm{PSI},i} = \frac{\min(0, -\beta_T^{\mathrm{N},i})}{\sum\limits_{\alpha=i,j,k}\min(0, -\beta_T^{\mathrm{N},\alpha})}, \tag{20}$$

where β^{N} is given by the N-scheme above.

Remark

Both the N-scheme and the PSI scheme are positive under the CFL condition

$$\Delta t_i^n \sum_{\{T/i\in T\}} \max(0, \vec{v}\cdot\vec{n}_i) \le 2|C_i|.$$

4.4. Lax–Wendroff and SUPG schemes

The SUPG and Lax–Wendroff schemes are also linearity preserving but are not positive. In the Lax–Wendroff scheme the distribution coefficients are given by

$$\beta_T^i \equiv \beta_T^{\mathrm{LW},i} = \tfrac{1}{3} + \frac{\Delta t_T}{|T|}\vec{v}\cdot\vec{n}_i,$$

where Δt_T is a constant cell time step and $|T|$ denotes the volume of triangle T. The choice of the nodal time step Δt_i and the cell time step Δt_T can be derived by generalization of a Fourier analysis on a Cartesian grid.

The fluctuation-splitting interpretation of the SUPG scheme is straightforward:

$$\beta_T^i \equiv \beta_T^{\mathrm{SUPG},i} = \tfrac{1}{3} + \frac{\tau}{|T|}\vec{v}\cdot\vec{n}_i,$$

where $\tau = ch_T/|\vec{v}|$ (c is a constant and h_T is a typical length scale of cell T). As seen from the expressions of $\beta_T^i \equiv \beta_T^{\mathrm{LW},i}$ and $\beta_T^i \equiv \beta_T^{\mathrm{SUPG},i}$, the SUPG scheme is identical to the Lax–Wendroff scheme for the choice $\tau = \frac{1}{2}\Delta t_T$ for a constant convection vector $\vec{v}$. The kinetic approach for these two schemes is discussed in more detail in Reference 15.

4.5. Finite element kinetic schemes

The finite element schemes for (10) are obtained[2,5,15] by multiplying (16) by the matrix vector $[V_1,V_2]$ and integrating over the velocity space $\mathrm{d}\vec{v}$. Indeed, this follows from the identities

$$W_i^n = \int_{\vec{v}\in\mathscr{R}^2} [V_1(\vec{v})f_i^n(\vec{v}) + V_2 g_i^n(\vec{v})]\,\mathrm{d}\vec{v},$$

$$W_i^{n+1} = \int_{\vec{v}\in\mathscr{R}^2} [V_1(\vec{v})f_i^{n+1}(\vec{v}) + V_2 g_i^{n+1}(\vec{v})]\,\mathrm{d}\vec{v},$$

$$\mathscr{F}_T^i(W_i^n) = \int_{\vec{v}\in\mathscr{R}^2} \vec{v}[V_1(\vec{v})\beta_T^i f_i^n(\vec{v}) + V_2\tilde{\beta}_T^i g_i^n(\vec{v})]\,\mathrm{d}\vec{v}.$$

The calculation of the flux $\mathscr{F}_T^i$ requires integrations

$$\int_E \beta_T^i v_1^m v_2^n\,\mathrm{d}v, \quad 0 \le n+m \le 3, \tag{21}$$

over

$$E = \{\vec{v}\cdot\vec{n}_i \ge 0,\ \vec{v}\cdot\vec{n}_j \ge 0\} \cap \mathscr{S} \quad (\mathscr{S} \text{ depends on the support of } \chi). \tag{22}$$

These integrals have to be calculated analytically. Here they have been simplified by considering only non-empty regions of intersection. All three possibilities were investigated and compared for the three multidimensional schemes considered here, i.e. the N-scheme (first-order), the PSI (second-order) scheme and the second-order (but non-positive) LDA scheme, while only the Dirac one was used for the PSI and LDA schemes. The comparisons proved that in most cases the Dirac distribution gave satisfactory results, improving the cost efficiency of such calculations as these intersection integrals then become redundant.

4.6. Positivity and entropy conditions

The kinetic schemes, whatever the choice of χ and ψ, must always be consistent and preserve positivity of density and pressure. The only choice of χ and ψ which meets this requirement and which yields a finite element scheme based on the kinetic approach preserving the entropy condition and the maximum principle for specific entropy is given by the equilibrium functions[3,15]

$$\chi(\vec{\omega}) = \alpha[1 - |\vec{\omega}|^2/\beta]_+^{\lambda}, \qquad \psi(\vec{\omega}) = \delta[1 - |\vec{\omega}|^2/\beta]_+^{\lambda+1},$$
$$\beta = 2 + \lambda, \qquad \alpha = \frac{1}{2\pi\beta\int_0^{\pi/2}\cos^{2\lambda+1}}, \qquad \delta = \frac{\lambda}{2\pi\beta\sum_0^{\pi/2}\cos^{2\lambda+3}.}$$

5. RESULTS

5.1. Shock reflection

The first test case concerns a non-grid-aligned oblique shock reflection for the three above schemes using the Dirac distribution in each case for the equilibrium functions. The Mach distributions are given in Figure 2. This shows the multidimensionality of the underlying schemes and that the precision is not affected by the use of the simpler Dirac function.

Taking a horizontal cut along the centreline and analysing the distribution of the entropy and Mach variables along this line, only the second-order non-positive LDA scheme is seen to oscillate across the shocks (Figure 3).

5.2. Ramp deflection test case

A good test case for testing properties of schemes for compressible flows with discontinuities shocks and contact discontinuities, is the flow over an angular bump in a canal.[16] In this case the N-scheme is calculated with all three possibilities for the function χ, i.e. circle, rectangle and Dirac distributions. The only marked difference was within the entropy distribution, which is more oscillatory for the Dirac distribution than for the circle or the rectangle. In the case of the circle the entropy distribution for the N-scheme was equivalent to that of the PSI scheme calculated using the Dirac choice. In all cases, i.e. LDA/Dirac, N-scheme/circle, rectangle, Dirac and PSI/Dirac, these levels are very low and excellent discontinuity capturing was obtained (Figure 4).

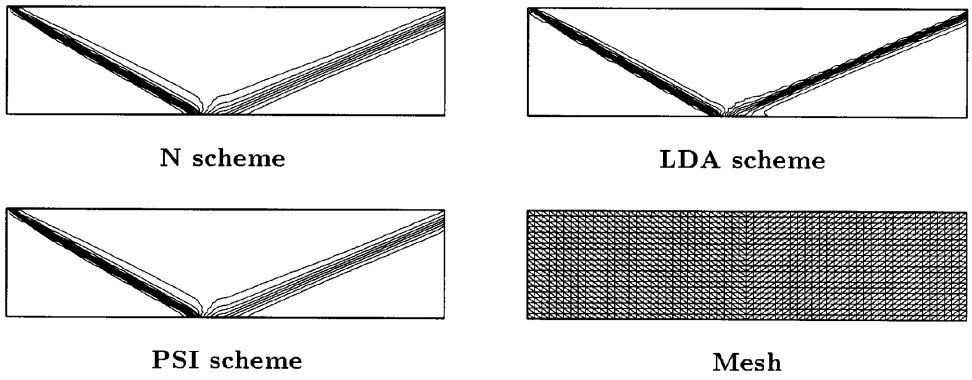

Figure 2. Mach number distribution for shock reflection

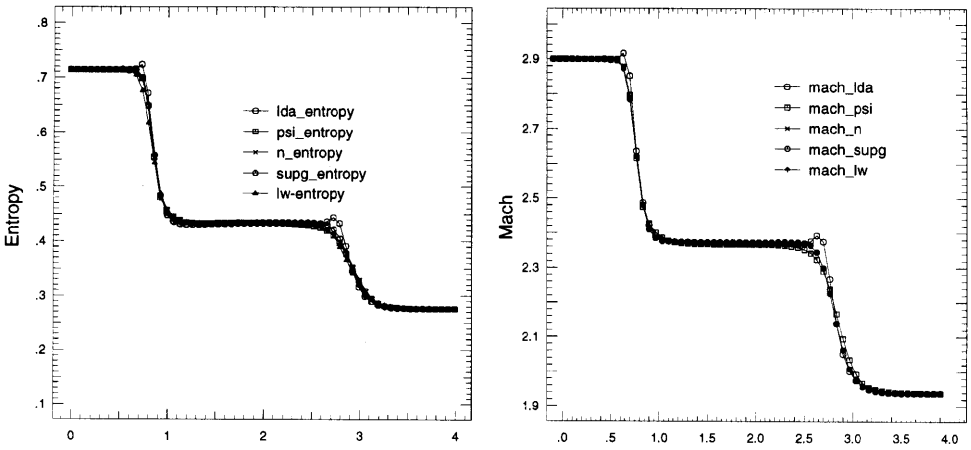

Figure 3. Entropy and Mach number distribution along mid-line for oblique shock reflection problem

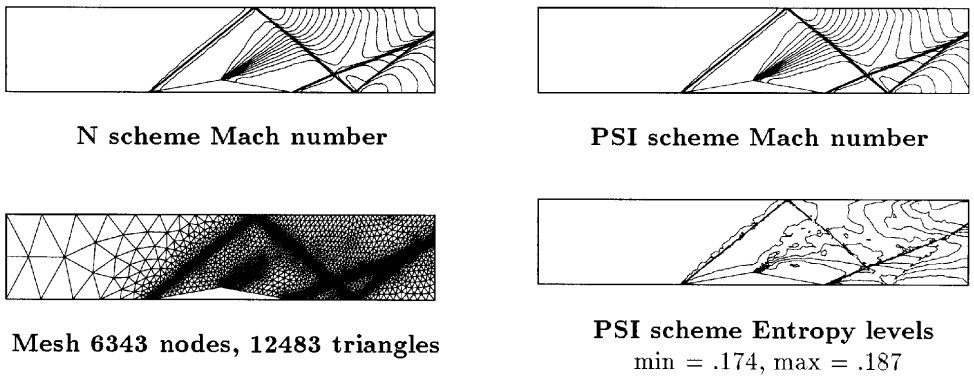

Figure 4. $M_\infty = 2$ flow over an angular bump

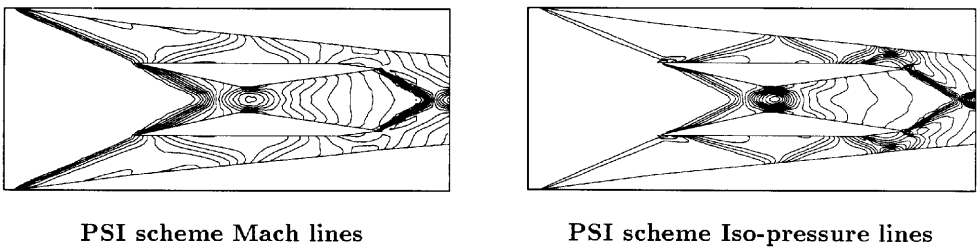

Figure 5. Solutions by kinetic PSI scheme for $M_\infty = 3{\cdot}6$ scramjet inlet flow

5.3. *Scramjet inlet flow*

The last test case shows the calculation of a supersonic flow, $M_\infty = 3{\cdot}6$, within a scramjet inlet on a non-adapted and irregular grid, illustrated in Figures 5 and 6. The extremely complex flow interactions and shock reflections are well captured by the kinetic schemes. Taking a fine and highly

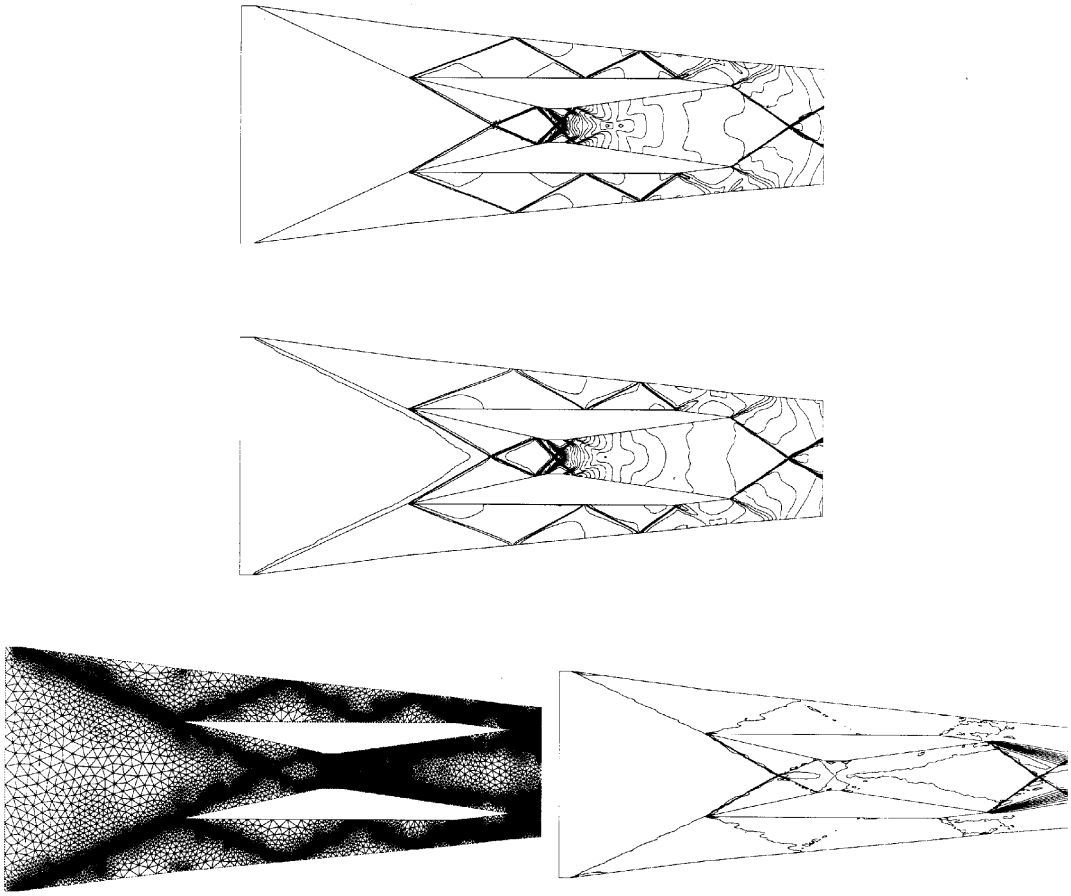

Figure 7. Kinetic fluctuation-splitting schemes for supersonic scramjet intake at Mach 3: LDA scheme (top) and N-scheme (centre). Entropy contours for N-scheme (bottom right) show entropy and linearity preservation. The mesh is a highly adapted one (bottom left)

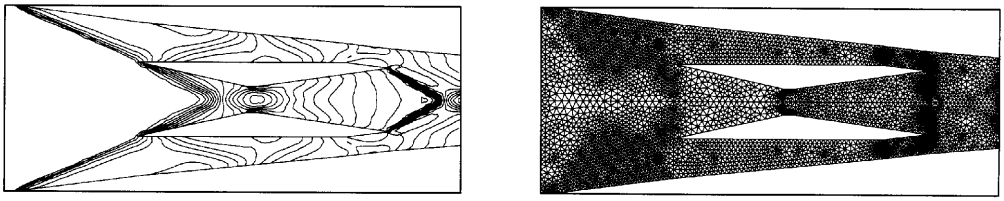

Figure 6. Iso-Mach lines by kinetic N-scheme for $M_\infty = 3{\cdot}6$ scramjet inlet flow (left) and corresponding coarse mesh (right)

adapted grid for a lower Mach number, $M_\infty = 3$, where multiple shock reflections occur between the components, the kinetic schemes prove to be highly accurate (Figure 7).

6. CONCLUSIONS

The extension of the kinetic approach for viscous (Navier–Stokes equations), reactive and also turbulent flows is now undertaken by several authors, but maintaining the complete Maxwellian for

the equilibrium functions in order to be able to rederive the equations. The possibility of using the approach developed here for the inviscid part and maintaining the other terms as source terms simplifies the complex integrals involved. The extension to other kinds of elements (quadrilaterals, prisms, hexahedra) is also possible. The combination of the kinetic approach with fluctuation splitting gives us very compact finite element schemes which yield robust results at least for supersonic and even for transonic flows. The schemes are not well adapted to subsonic flows, however, and their modification to handle such zones is now underway.

ACKNOWLEDGEMENTS

The authors have worked closely with Benoit Perthame and Bruno Stoufflet on these issues. The work was partially financed by a CEE HCM programme, together with the Swiss Federal office for higher education (OFES).

REFERENCES

1. H. Deconinck, R. Struijs, G. Bourgois and P. L Roe, 'Compact advection schemes on unstructured grids', *VKILS 1993-04*, 1993.
2. S. M. Desphande, 'A second order accurate, kinetic theory based, method for inviscid compressible flows', *NASA Tech. Paper 2613*, 1986.
3. B. Khobalatte and B. Perthame, 'Maximum principle of the entropy and second order kinetic schemes', *J. Math. Comput.*, **62**, 119–131 (1994).
4. B. Perthame, 'Second order Boltzmann schemes for compressible Euler equations in one or two space variables', *SIAM J. Numer. Anal.*, **29**, 1–19 (1992).
5. D. U. Pullin, 'Direct simulation methods for compressible inviscid ideal gas flow', *J. Comput. Phys.*, **34**, 231–244 (1980).
6. K. Xu, 'Numerical Navier–Stokes from gas kinetic theory', *J. Comput. Phys.*, **114**, 9–17 (1994).
7. W. M. Eppard and B. Grossman, 'A multidimensional kinetic-based, upwind solver for the Euler equations', *AIAA paper 93-3303-CP*, 1993.
8. B. Khobalatte and P. Leyland, 'Résolution des équations de la dynamique des gaz par des schémas de "fluctuation-splitting" utilisant les méthodes cinétiques', *IMHEF Rep.* T-97-4, November 1994.
9. B. Perthame, Y. Qiu and B. Stoufflet, 'Sur la convergence des schémas "Fluctuation–Splitting" pour l'advectron" CRA S Paris, Série I, 319, pp 283–288, *Note C.R. Acad. Sci. Paris*, (1994).
10. J. P. Boris and D. Book; 'Flux corrected transport', *J. Comput. Phys.*, **11**, 64–69 (1973).
11. R. H. Ni, 'A multiple-grid scheme for solving the Euler equations', *AIAA J.*, **20**, 1565–1571 (1982).
12. P. L. Roe, 'A conservative linearisation of the multidimensional Euler equations', Technical report, Cranfield, CoA8910, 1989.
13. P. L. Roe and D. Sidilkover, 'Optimum positive linear schemes for advection in two and three dimensions', *SIAM J. Numer. Anal.*, **29**, 1505–1825 (1992).
14. D. Sidilkover, 'Numerical solution to steady state problems with discontinuities', *Ph.D. Thesis*, Weizmann Institute of Science, Rehovot, 1989.
15. B. Khobalatte and P. Leyland, 'Linearity preserving kinetic schemes for the solution of the Euler equations on unstructured meshes', IMHEF T-97–14, August 1996.
16. R. Richter and P. Leyland, 'Entropy correcting schemes and non-hierarchical auto-adaptive dynamic finite element type meshes: applications to unsteady aerodynamics', *Int. J. numer. methods fluids*, **20**, (1995).

